

Analysis of Microstructural Changes during Pulsed CO₂ Laser Surface Processing of AISI 316L Stainless Steel

E. Chikarakara^{1,a}, S. Naher^{1,b} and D. Brabazon^{1,c}

¹Materials Processing Research Centre, Dublin City University, Dublin 9, Ireland

^aevans.chikarakara2@mail.dcu.ie, ^bsumsun.naher@dcu.ie, ^cdermot.brabazon@dcu.ie

Keywords: CO₂ pulsed laser processing, surface microstructure, melt pool size, surface roughness analysis

Abstract. In the present contribution, a 1.5kW CO₂ laser in pulsed wave mode was used to study the effects of laser processing parameters at specific energy fluence. Cylindrical AISI 316L stainless steel samples rotating perpendicular to the laser irradiation direction were used for these experiments. A surface temperature prediction model was implemented to set the experimental process parameters. Laser processing of AISI 316L steel showed a strong correlation between melt pool depth and the residence time at specific fluence levels. At fixed energy fluence, increase in residence time resulted in growth of the melt pool depth. In the melted region, the microstructure was observed to be of more uniform composition and contain fewer impurities. To improve absorption level, samples were etched and roughened. These samples exhibited lower roughness levels compared to the un-treated samples. For a constant fluence level, samples with improved absorption displayed an increase in depth of melt pool at lower peak powers and higher residence time. As the laser beam interaction time increased, the surface roughness of the steel increased for the various pulse energy levels examined. While the structure of the surface was seen to retain a crystal arrangement, grain orientation changes were observed in the laser processed region.

Introduction

AISI 316L stainless steel has various uses across the engineering spectrum owing to its high corrosion and wear resistance properties. Applications include surgical instruments, food storage containers and pipelines. Improvements of the tribological properties have recently been exploited through various laser surface engineering techniques [1-3]. Laser surface modification techniques including laser glazing, re-melting and cladding involve highly localised interaction between the laser beam and substrate. The laser glazing process involves irradiating the surface in order for melting to just commence locally within the spot region. This would assist in rapid solidification of the material and should result in reduced roughness compared to higher fluence levels. This can offer huge benefits in terms of wear and corrosion resistance properties compared to conventional surface coating methods [4].

Advantages of laser processed surfaces for tribological properties include:

- i. A resultant structure without porosity;
- ii. Superior bonding with the substrate. This quality is crucial for wear and corrosion resistant applications as it prevents failure at the interface, which is a vital constraint within convectional coated material;
- iii. Oxidation effects can simple be eliminated through the use of an inert assist gas i.e. argon. High vacuum conditions are thus not required making the manufacturing facile compared to other techniques;
- iv. Specific areas can be processed without affecting surrounding areas hence permitting for critical regions of interest of a component requiring improvement to be processed. This demonstrates high flexibility and precession;

- v. Depth of processing can easily be controlled and the heating effect is highly localised therefore bulk mechanical properties are left unchanged;
- vi. Less time/energy and material required compared to convectional coating techniques;
- vii. Little or no surface preparation is necessary [5].

Among the notable advantages, laser surface engineering enables delivery of a controlled energy with precise temporal and spatial distribution. A by-product of this process is an extremely fast heating/cooling rate, very high thermal gradient and rapid re-solidification velocity. These extreme processing conditions very often develop a unique microstructure and composition in the near surface region with large extension of solid solubility and formation of metastable even amorphous phases. Amorphisation of the surface layer of a stainless steel is desirable as it is known to improve the wear and corrosion resistance as well as eliminate intercrystalline defects within the microstructure [6].

Some of the characteristics that affect the application of laser surface engineered material include, depth of processing, overlapping effects or homogeneous distribution of the processed region and surface roughness. Presently, little research has been undertaken on pulsed laser treatment and its effects on the microstructure melt pool formation, surface roughness and crystallinity changes. This research is crucial in designing and predicting the surface structure of the processed material. This contribution explores the direct effect of laser parameters on the surface microstructure structure of AISI 316L stainless steel.

Experimental and Model Set Up

Material Preparation and Design of Experiments: AISI 316L austenitic stainless steel, with elemental composition given in Table 1, was used in this investigation. Samples were cut into cylindrical sections 120mm long and 10mm in diameter. Absorbance of CO₂ irradiation by steel surfaces is known to be dependent on surface roughness [7-9]. The samples were machined and etched to improve the absorption.

Table 1: Chemical composition of AISI 316L stainless steel

Element	Cr	Ni	Mo	Mn	Si	Co	N	S	P	C	Fe
Wt%	16.82	10.14	2.03	1.51	0.55	0.08	0.061	0.03	0.03	0.02	Bal.

Laser Treatment: A 1.5kW, 10.6μm wavelength, CO₂ laser operating in pulsed mode was used for irradiating the samples. Argon gas at 1 bar pressure shielded the melt pool thus avoiding oxidation. The sample was rotated using a DC motor fixed to a table that moved perpendicular to the laser irradiation direction. Fig. 1 shows a schematic of the laser modification process. The laser beam was kept perpendicular to the workpiece during laser irradiation to maximise the absorbance and ensure uniform conditions for processing [8].

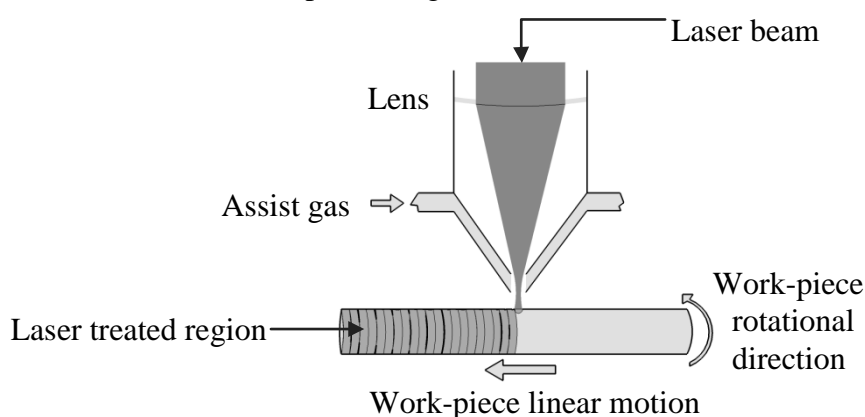


Figure 1: Schematic of the laser processing set-up

Tangential and linear velocities were kept constant at 270mm/s and 46mm/min respectively, in order to keep the surface spot overlap constant at 0%. A 90 μm spot diameter was used for all the experiment runs by focusing the Gaussian beam on the surface of the workpiece. The pulse repetition frequency was kept constant at 3 kHz so as to control the residence time by varying the duty cycle independently. Residence time, R, is the equivalent of exposure time for continuous mode lasers and can be calculated as follows [11]:

$$R = \frac{\tau \times D_b \times PRF}{v} \quad (1)$$

where τ is the pulse width (s), D_b is the diameter of the beam spot (m), PRF is the pulse repetition frequency (Hz) and v is the scan speed (m/s).

As the overlap was set to 0% for the experimental work presented, the residence time is equivalent to the pulse width. To comprehend the effects of peak power and pulse duration, parameters summarised in Table 2 were investigated. The laser parameters were selected based on screening experiments in order to just melt the surface. In this design of experiments the fluence was set at two levels by varying power and residence times accordingly. Three surface pre-treatments techniques were used resulting in 15 experimental conditions being investigated. The machined pre-treatment consisted of machining ridges with a Ra value of approximately 3 μm . Glyceregia etchant was applied to dull the steel surface, hence increasing the CO₂ laser absorbance [10]. Samples were cleaned and rinsed with acetone prior to the laser treatment.

Characterisation: Cross sectional views were prepared by sectioning the sample perpendicular to the longitudinal axis. Samples were polished and etched, again using glyceregia, to reveal the grain boundaries for microscopy. Microstructure analysis was carried out using the scanning electron microscope (SEM), Carl Zeiss, EVO LS15. Element analysis and chemical characterisation was performed with an energy dispersive x-ray spectrometer (EDX), Inca X-Act and Microanslysis suit, Oxford Instruments. The Beuhler Omnimet image analysis software incorporated with the Reichart Me F2 optical microscope was used to obtain the average meltpool depth. Phase and crystallinity analysis was investigated using a Cu-K α radiation X-ray diffractometer (XRD). Scanning was performed at 0.1°/min, varying the diffraction angle between 15 and 110°. Surface roughness measurements were performed using a stylus profilometer, Civil Instruments TR200, with stylus tip radius of 2 μm . Sampling and evaluation lengths used were 0.8 mm and 4 mm respectively. The roughness was measured according to ISO 4287/4288.

Thermal Model: In order to obtain the pulse energy required to just barely reach the required melting point two methods, i) process mapping and ii) thermal prediction, were implemented. Surface temperature induced by the laser beam can be estimated using the Equation 2 [3, 12]:

$$T = \frac{q\eta}{r_b} \left[0.147 - 0.054 \ln\left(\frac{Vr_b}{4\alpha}\right) \right] \quad (2)$$

where T is the surface temperature (°C), η is absorption coefficient (dimensionless unit), q is laser average power (W), V is scan speed (m/s), r_b is beam radius (m), α is the thermal diffusivity (m²/s).

Absorption coefficient of 316L stainless steel is estimated between 0.02 and 0.051 [8]. Absorption coefficient values correspond to the 98% and 94.1% reflectivity of highly polished and roughened samples for a CO₂ laser wavelength of 10.6 μm . In this study the absorption coefficient was estimated to be 0.035 for the non treated steel. It should be noted that the above equation was created for continuous mode therefore it does not take into account the duty cycle to obtain interaction time.

A linear relationship is observed between predicted temperature and average power since pulse duration is not accounted for and the scanning speed and beam spot size are kept constant for all

experimental runs. Fig. 2 illustrates surface temperature predictions from Equation 2 for varying average power used in this work. The prediction maps the average power required to reach certain temperatures on the surface of the workpiece. This method predicts melting at an average power of 220W which corresponds to 1153 J/cm^2 .

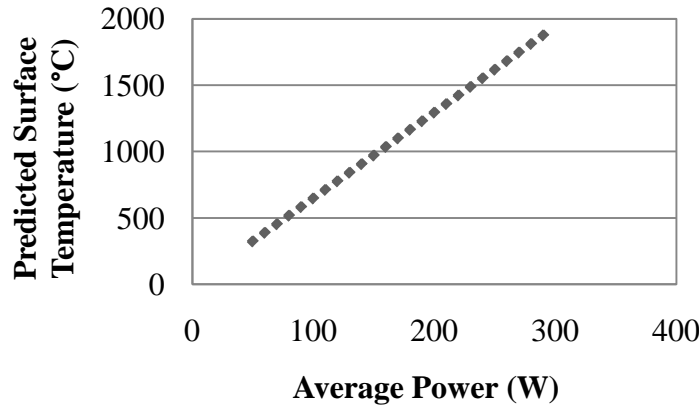


Figure 2: Surface temperature prediction from thermal model.

Results and Discussion

Microstructure Analysis: A process mapping experiment was carried out with energy fluence ranging between 500 and 2500 J/cm^2 . Fig. 3 shows the findings of the process mapping experiment highlighting insufficient energy.

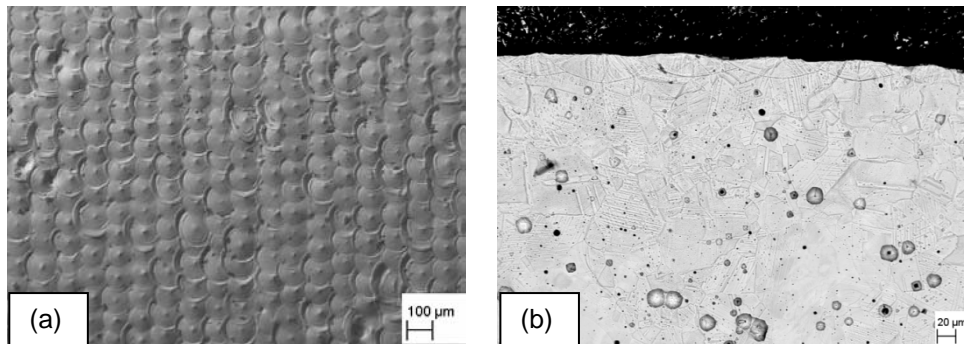


Figure 3: Influence of low energy fluence 500 J/cm^2 on melting of surface
a) surface topology and b) cross sectional microstructure

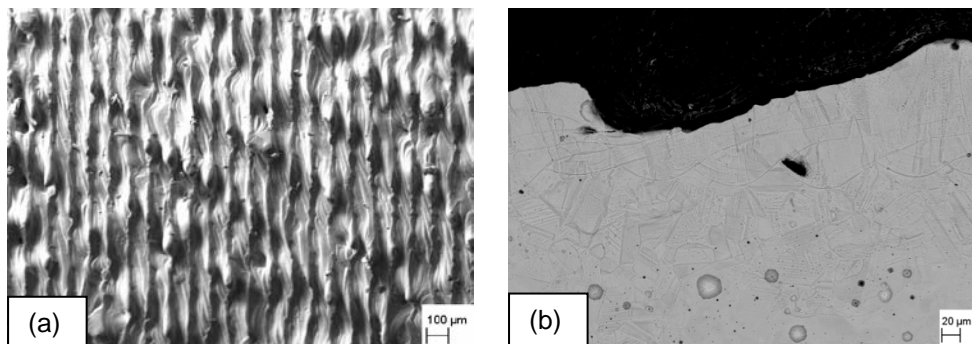


Figure 4: Influence of high energy fluence 1500 J/cm^2 on melting of surface
a) surface topology and b) cross sectional microstructure

Fig. 3 demonstrates low laser energy outputs (500 J/cm^2) that result in insufficient surface melting thus showing laser marking effects. The laser marking effect is caused by localised melting. Laser

spot shapes produced are attributed to the Gaussian characteristics of the laser beam. Negligible overlap occurred since relatively small amount of melting occurred therefore the initially set spot size is visible. There is no evident change in microstructure as can be seen in Fig. 3 (b).

Increasing the pulse energy to 1500 J/cm^2 produces ablation on the surface of the steel as shown in Fig. 4 (a). The ablation can easily be noticed through the formation of distorted channel-like features on the steel. Fig. 4 (b) shows the corresponding microstructural effects and material removal on the steel surface. Overlapping of the spots is visible and this is attributed to high irradiance producing melting pools larger than the initially set laser beam diameter.

A study was undertaken to investigate changes in microstructure for fixed energy fluence. The topography of the samples laser modified using similar energy fluence (1048 J/cm^2) but with different peak powers and pulse durations are shown in Fig. 5 and Fig. 6. Fig. 5 (a) shows the treated surface at 1 kW peak power and $67 \mu\text{s}$ residence time. Fig. 5 (b) shows the surfaces processed with 0.4 kW peak power and $167 \mu\text{s}$ residence time. Fig. 6 show the cross sectional views corresponding to Fig. 5. Lower exposure time produced less surface melting and hence a smoother surface morphology. The morphology exhibited in Fig 5 and Fig 6 (b) show an enlarged melted phase due to a higher exposure time owing to the higher residence time. This is evident from the melt pool depth and roughness results shown in Table 2.

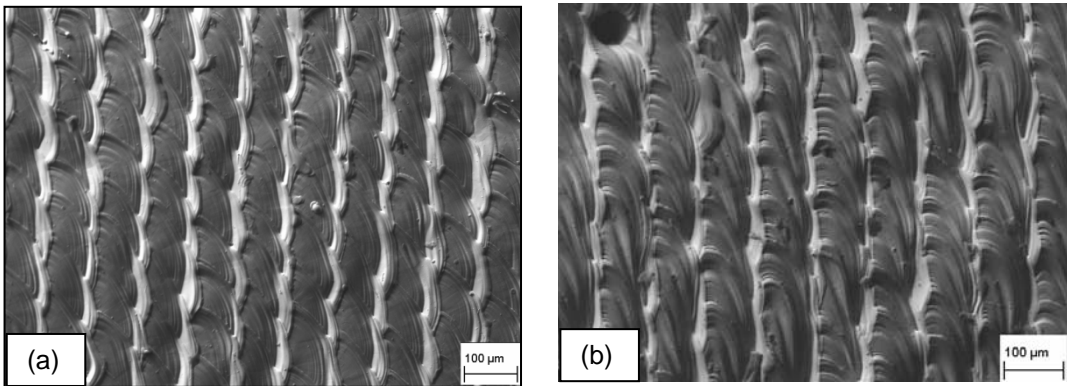


Figure 5: SEM micrograph of the laser modified steel surface made using a fixed energy fluence (1048 J/cm^2) with: a) high peak power (1 kW) and low residence time ($67 \mu\text{s}$);
b) low peak power (0.4 kW) and high r ($167 \mu\text{s}$)

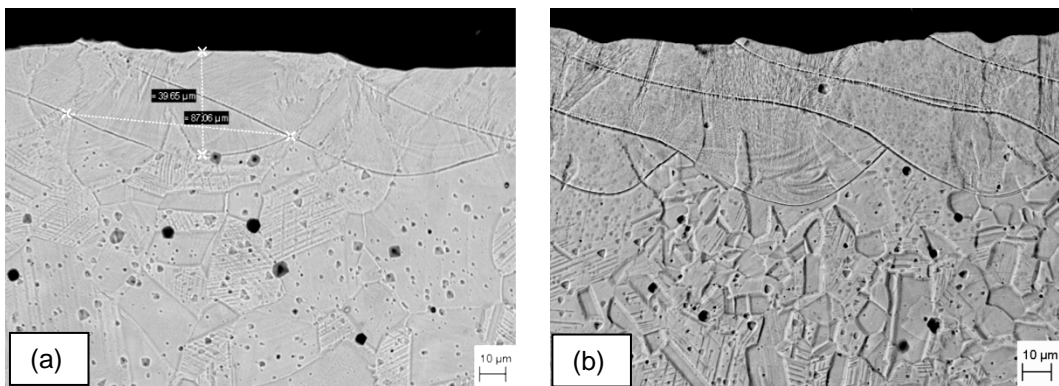


Figure 6: Back scatter SEM images of transverse cross sectional microstructure corresponding to processed surface shown in Fig. 5 (a) and (b)

Glyceregia etchant reveals carbide formation within the stainless steel microstructure. The small dark spots visible within the microstructure in Fig. 6 (a) and (b) resemble carbides in the steel. However these phases are not present within the laser processed region. Creation of a chemically uniform and defect free surface is useful as it can lead to increased wear resistant surfaces [13].

Table 2: Melt pool depth and roughness measurements obtained from the experiment

Peak Power (W)	Pulse Width (μs)	Energy Fluence (J/cm ²)	Surface Temp. (°C)	No Pre-treatment		Machined		Machined and Etched	
				Depth (μm)	Roughness (μm)	Depth (μm)	Rough. (μm)	Depth (μm)	Roughness (μm)
1000	67	1048	1292	45	2.14	43	2.40	72	3.35
800	83	1048	1292	47	2.42	56	2.79	55	2.79
400	167	1048	1292	55	3.63	90	3.38	59	3.38
700	100	1100	1357	57	6.90	88	12.00	75	4.01
1400	50	1100	1357	55	4.00	51	3.35	46	2.23

Melt Pool Size Analysis: Interaction of melt pool depth to peak power and pulse width

Size of the melt pool can be related to the peak power and residence time given that energy fluence is kept constant. Table 3 shows the melt pool depth and roughness measured for the specific processing conditions investigated. At the higher peak power (1 kW) and low residence time (67 μs) a depth of approximately 40 μm was observed; see Fig. 6 (a). More than double the depth of altered microstructure (approximately 90 μm) was observed for the same energy fluence but different pulse parameters see Fig. 6 (b). Fig. 7 shows the relationship between residence time and melt pool depth using same energy fluence. Melt pool depth increases as the residence time increases.

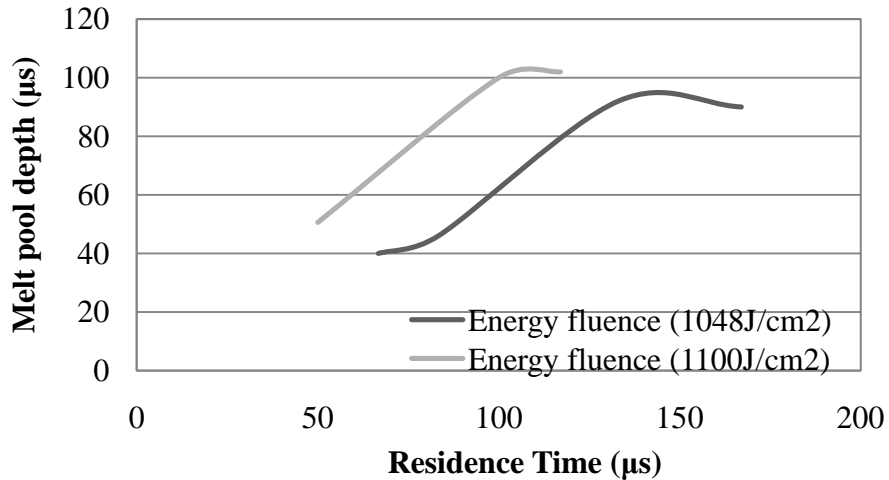


Figure 7: Interaction of melt pool depth to residence time

Laser parameters interaction on overlapping: Overlap parameters were set to 0%, however overlapping is still visible on the samples, see Fig. 6. This was due to the heat diffusion within individual melt pools that result in the subsequent laser pulse directly irradiating the previous melt pool or heated region. The temperature gradient and different cooling rates forged a boundary creating overlaps visible in Fig. 6. Centrifugal force due to sample rotation was a significant contributing factor to the overlapping features observed on the microstructural images.

Effects of laser peak power and surface pre-treatments on melt pool depth: Fig.8 highlights the effect of the laser peak power, residence time and surface pre-treatment at a fixed energy fluence of 1048J/cm². The pre-treated surface has a larger melt pool depth compared to the non pre-treated samples. This is due to the higher surface roughness and increase in irradiation absorption of the material. Pre-surface treatment methods had a significant impact on depth of processing at low peak power and higher residence time. A negligible effect was evident at high peak power and low resident times due to the reduced interaction time of the laser and work piece.

Depth of processing decreases with reduction of the residence time. The residence time determines the duration at which the beam is in contact with sample thus decrease in residence time reduces results in lower depth of processing. Since the energy fluence is fixed therefore peak power increase relates to a lower melt pool depth.

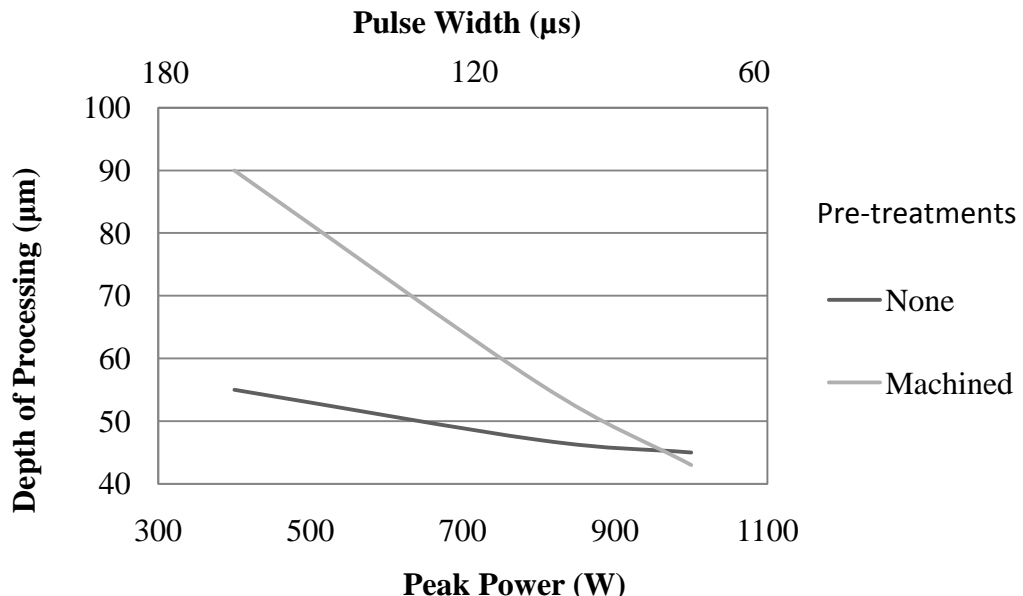


Figure 8: Effects of peak power on the depth of processing

Roughness Analysis: An analysis of the effects of laser processing parameters on average roughness of the sample was carried out. Fig. 9 (a) shows the roughness produced by the laser irradiation when the sample had been subjected to different pre-treatments.

Pre-treated samples produced higher roughness measurements, up to 14 μm mainly due to the machining done prior to laser processing. Low roughness results below 600W were caused by insufficient melting of the surface. Resulting roughness of the samples can be correlated to the residence time as shown in Fig. 9 (b). Fig 9 (b) shows an increase in roughness as the residence time is increased. Increase in residence time periods results in longer interaction between laser and surface of material. This intensifies melting of the surface and delays the cooling rate consequently resulting in rougher steel surfaces.

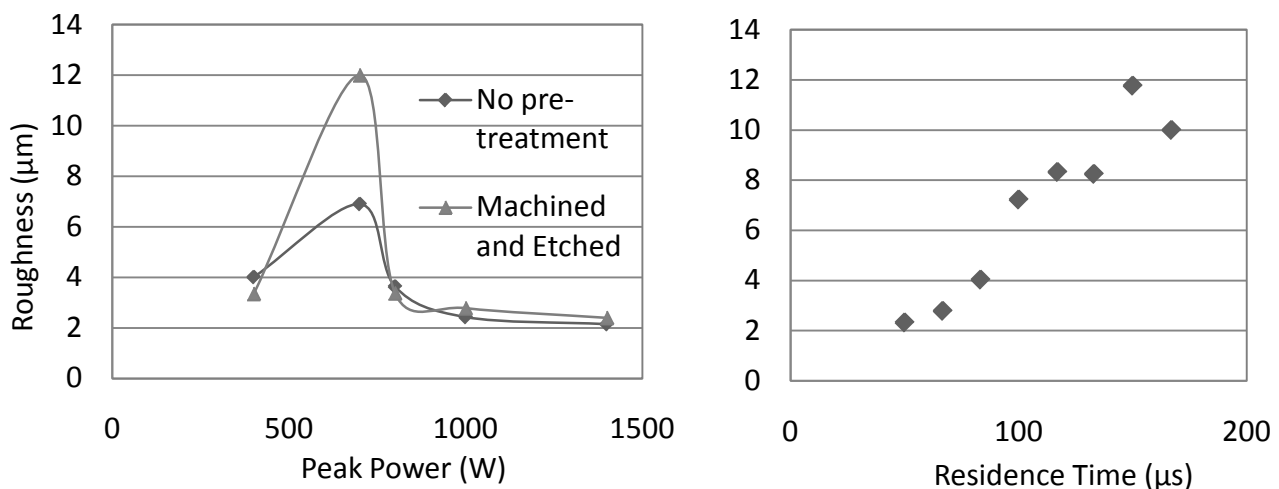


Figure 9: Effects of (a) surface pre-treatment and power; (b) residence time on roughness

Conclusion

Surface thermal prediction method can be used to predict the energy fluence required to melt the surface of the steel. Microstructure analysis of the surface revealed overlapping at temperatures above the melting temperature of steel. More uniform chemical composition was observed in the laser treated regions. Melt pool depth was influenced by resident time, pre-treatment and energy fluence. Increased pulse width resulted in a rise of the melt pool depth at a fixed level of energy fluence. Increasing the energy fluence also resulted in enhanced depth of processing. Machined surfaces and high exposure times resulted in higher melt pool depth at low peak powers compared to non-treated surfaces. A correlation between roughness and surface pre-treatments was observed. With machined and etched samples exhibiting higher roughness compared to untreated surfaces. No crystalline changes were identified using the XRD on the laser modified surfaces. It is likely that this was due to the relatively long residence time used in the experiments.

References

- [1] N. Parvathavarthini, R. V. Subbarao, S. Kumar, R. K. Dayal and H. S. Khatak., Journal of Materials Engineering and Performance 10(1), (2001) p. 5-13).
- [2] F. Laroudie, C. Tassin and M. Pons, Journal De Physique 4(4), (1994), pp. 77-80.
- [3] A. Viswanathan, D. Sastikumar, P. Rajarajan, H. Kumar and A. K. Nath, Opt. Laser Technol. 39(8) (2007), pp. 1504-1513
- [4] C. T. Kwok, F. T. Cheng and H. C. Man. Cavitation erosion and corrosion behaviour of laser surface melted 316L stainless steel (1997)
- [5] W. M. Steen and K. G. Watkins. Coating by laser surface treatment, Journal De Physique IV (1993), p. 581
- [6] J. D. Majumdar and I. Manna, Laser processing of materials, Sadhana (2003) p. 495–562
- [7] D. Bergström, J. Powell and A. F. H. Kaplan, Appl. Surf. Sci. 253(11), (2007), p. 5017-5028
- [8] T. Mahank, Laser glazing of metals and metallic and ceramic coatings, Vol. 1, 2004, p. 26
- [9] P. A. A. Khan and T. Debroy. Absorption of CO₂ laser beam by AISI 4340 steel. Metallurgical Transactions B 16(4), (1985), p. 853
- [10]J. H. Abboud, K. Y. Benyounis, A. G. Olabi and M. S. J. Hashmi, J. Mater. Process. Technol. 182(1-3), p. 427-431(2007)
- [11]A. N. Samant, S. P. Harimkar and N. B. Dahotre, J. Appl. Phys. 102(12), (2007)
- [12]J. S. Selvan, G. Soundararajan and K. Subramanian, Surface and Coatings Technology 124 (2-3), (2000) p. 117-127
- [13]Information on <http://pwatlas.mt.umist.ac.uk/internetmicroscope//micrographs/microstructures/low-carbon-steel.html>